Formation of sulfur atomic layers on gold from aqueous solutions of sulfide and thiosulfate: Studies using EC−STM, UHV−EC, and TLEC

ARTICLE *in* LANGMUIR · AUGUST 2003

Impact Factor: 4.46 · DOI: 10.1021/la034474y

3 AUTHORS, INCLUDING:

John L. Stickney
University of Georgia
177 PUBLICATIONS **3,358** CITATIONS

Formation of Sulfur Atomic Layers on Gold from Aqueous Solutions of Sulfide and Thiosulfate: Studies Using EC-STM, UHV-EC, and TLEC

Marcus D. Lay, Kris Varazo, and John L. Stickney*

Department of Chemistry, University of Georgia, Athens, Georgia 30602

Received March 18, 2003. In Final Form: June 20, 2003

The formation of S atomic layers on Au from alkaline solutions of sulfide and thiosulfate is described. These studies are relevant to the formation of self-assembled monolayers (SAMs), as sulfide can be thought of as the simplest thiol and, thus, S atomic layers as the shortest chain SAM. S atomic layers are also of interest as precursors for the electrochemical formation of compound semiconductor thin films such as ZnS, CdS, and PbS. The deposition of S was investigated using electrochemical scanning tunneling microscopy (EC-STM), thin layer electrochemistry (TLEC), and ultrahigh vacuum electrochemical techniques (UHV-EC). UHV-EC studies included analysis with Auger electron spectroscopy (AES), low energy electron diffraction (LEED), and X-ray photoelectron spectroscopy (XPS). EC-STM and LEED revealed a $^1/_3$ coverage $(\sqrt{3} \times \sqrt{3})R30°$-S structure, previously observed by a number of workers, formed from both sulfide and thiosulfate solutions. From sulfide solutions, EC-STM showed that the $(\sqrt{3} \times \sqrt{3})R30°$-S structure converted to a more complex $(3\sqrt{3} \times 3\sqrt{3})R30°$-S structure at higher potentials, with an accompanying surface roughening transition. LEED indicated the formation of a structure with a (2×2) unit cell near bulk deposition potentials in sulfide and thiosulfate solutions. EC-STM studies in thiosulfate solutions evinced this (2×2) structure, apparently composed of S dimers. Initial immersion into the thiosulfate solution resulted in a structure with a $c(4 \times 2\sqrt{3})$ unit cell, believed to contain adsorbed thiosulfate species. The $c(4 \times 2\sqrt{3})$ structure was replaced by the $(\sqrt{3} \times \sqrt{3})R30°$-S structure via reduction, as thiosulfate can be reductively decomposed to produce sulfide. In general, sulfide can be oxidized at fairly low potentials to form an adsorbed sulfur atomic layer, initially the $(\sqrt{3} \times \sqrt{3})R30°$-S structure on Au(111), a process referred to as oxidative underpotential deposition (upd). Bulk deposits of sulfur and possibly polysulfides are formed at more positive potentials.

Introduction

The power of scanning tunneling microscopy (STM) for resolving surface structures with atomic resolution is presently unmatched. Atomic resolution STM studies have been successfully carried out in a vacuum,[1,2] under ambient conditions,[3] and in solution.[4] A major constraint is the need for a conducting substrate. However, this is not a problem in electrochemical studies, as electrodes are generally highly conductive. Therefore, electrochemical scanning tunneling microscopy (EC-STM) has proven to be an invaluable tool for the in-situ investigation of atomic scale processes at the solid/liquid interface; it provides a real space image, elucidating the repeating unit of the lattice (unit cell), the arrangement of atoms within (basis), and morphology changes, up to the micron scale.

Elemental, structural, and oxidation state information can be obtained using ultrahigh vacuum electrochemical techniques (UHV-EC)[5] such as Auger electron spectroscopy (AES), low energy electron diffraction (LEED), and X-ray photoelectron spectroscopy (XPS), respectively. UHV-EC involve the emersion (withdrawal) and transfer of the electrode from solution to a surface analysis chamber, while minimizing exposure to ambient conditions. The electrochemistry and electrode transfer are performed in an ultrahigh purity (UHP) inert gas and in a vacuum, respectively. However, even UHP inert gas has a significant amount of oxygen. Additionally, changes in surface structure and composition may occur when potential control is lost during the emersion process. This often becomes an issue when using potentials below that for hydrogen evolution and/or with highly reversible systems.[6] However, the chalcogenides have proven to work well in UHV-EC studies, partly as a result of the irreversibility of their deposition.[7]

The studies here are concerned with electrochemically forming and describing atomic monolayers of S on Au(111) surfaces. There are a number of important compounds which contain S, such as PbS, CdS, ZnS, $CuInS_2$, and HgS, thus making the formation of an atomic layer of S a central issue for our work. The formation of sulfur atomic layers on metallic single crystal surfaces has been widely studied: Au,[8−16] Pt,[17−24] Ni,[25−28] Rh,[29−31] Pd,[32−36] and Ru.[37−41] Sulfur atomic layers play an important role in

* To whom correspondence should be addressed. E-mail: stickney@sunchem.chem.uga.edu.

(1) Barth, J. V.; Brune, H.; Ertl, G.; Behm, R. J. *Phys. Rev. B* **1990**, *42*, 9307−9318.
(2) Woll, C.; Chiang, S.; Wilson, R. J.; Lippel, P. H. *Phys. Rev. B* **1989**, *39*, 7988−7991.
(3) Mizutani, W.; Ohi, A.; Motomatsu, M.; Tokumoto, H. *Appl. Surf. Sci.* **1995**, *87*−*8*, 398−404.
(4) Tao, N. J.; Lindsay, S. M. *J. Appl. Phys.* **1991**, *70*, 5141−5143.
(5) Soriaga, M. P.; Stickney, J. L. In *Modern Techniques in Electroanalytical Chemistry*; Vanysek, P., Ed.; Wiley & Sons: New York, 1996; p 1.
(6) Lay, M. D.; Varazo, K.; Srisook, N.; Stickney, J. L. *J. Electroanal. Chem.*, in press.
(7) Ocko, B. M.; Magnussen, O. M.; Adzic, R. R.; Wang, J. X.; Shi, Z.; Lipkowski, J. *J. Electroanal. Chem.* **1994**, *376*, 35−39.
(8) Kostelitz, M.; Oudar, J. *C. R. Acad. Sci., Ser. C* **1970**, *271*, 1205.
(9) Kostelitz, M.; Oudar, J. *Surf. Sci.* **1971**, *27*, 176.
(10) Kostelitz, M.; Domange, J. L.; Oudar, J. *Surf. Sci.* **1973**, *34*, 431−449.
(11) Gao, X. P.; Zhang, Y.; Weaver, M. J. *J. Phys. Chem.* **1992**, *96*, 4156−4159.
(12) Demir, U.; Shannon, C. *Langmuir* **1994**, *10*, 2794−2799.
(13) Bondzie, V.; Dixon-Warren, S.; Yu, Y. *J. Chem. Phys.* **1999**, *111*, 10670−10680.
(14) Andreasen, G.; Vericat, C.; Vela, M. E.; Salvarezza, R. C. *J. Chem. Phys.* **1999**, *111*, 9457−9460.

10.1021/la034474y CCC: $25.00
Published on Web 08/13/2003

corrosion processes,[42,43] in poisoning catalysis,[44−47] and in the electrochemical formation of sulfur containing compound semiconductor thin films.[12,48−56] Additionally, in the area of self-assembly, or self-assembled monolayers (SAMs), thiols are a main protagonist. Sulfide can be thought of as the smallest thiol, and a sulfide layer can be thought of as the shortest chain SAM.

The compound electrodeposition method used in this group is referred to as electrochemical atomic layer epitaxy (EC-ALE). EC-ALE is a method for electrodepositing compound semiconductors one monolayer at a time.[57−59] It is the electrochemical analogue of atomic layer epitaxy (ALE).[60−63] ALE is based on the use of surface-limited reactions to promote two-dimensional growth and form materials layer-by-layer, with the number of cycles determining the thickness of the deposit. In electrodeposition, surface-limited reactions are generally referred to as underpotential deposition (upd);[57,64−67] this process involves an atomic layer of a species depositing on another at a potential prior to that required for the species to deposit on itself. In EC-ALE, thin films are formed by the sequential upd of each element from a separate solution. Several groups have prepared thin films of CdS and ZnS compound semiconductors using EC-ALE.[12,48−56,68] CdTe, CdSe, and ZnSe have also been prepared.[69−78] There are recent reports of the EC-ALE formation of the III−V compounds InSb and InAs and IV−VI compounds such as PbSe and PbTe, as well as superlattices of these compounds.[79,80] The first cycle of compound deposition turns out to be the most difficult to control and the most important. Thus, knowledge of the structure and composition of the first atomic layer of S becomes critical to control of the deposit structure.

EC-STM has been extensively applied to the characterization of sulfur atomic layers on Au(111). Sulfide oxidation on Au(111) electrodes was studied by Weaver et al. using EC-STM.[11] In acidic solutions containing 1 mM Na_2S, a $^1/_3$ ML ($\sqrt{3} \times \sqrt{3}$)*R*30° unit cell was observed between −0.4 and −0.1 V vs SCE, with sulfur atoms in

(15) Vericat, C.; Andreasen, G.; Vela, M. E.; Salvarezza, R. C. *J. Phys. Chem. B* **2000**, *104*, 302−307.
(16) Martin, H.; Vericat, C.; Andreasen, G.; Creus, A. H.; Vela, M. E.; Salvarezza, R. C. *Langmuir* **2001**, *17*, 2334−2339.
(17) Berthier, Y.; Perdereau, M.; Oudar, J. *Surf. Sci.* **1973**, *36*, 225−241.
(18) Heegemann, W.; Bechtold, E.; Hayek, K. *Jpn. J. Appl. Phys.* **1974**, 185−187.
(19) Heegemann, W.; Meister, K. H.; Bechtold, E.; Hayek, K. *Surf. Sci.* **1975**, *49*, 161−180.
(20) Fischer, T. E.; Kelemen, S. R. *Surf. Sci.* **1977**, *69*, 1−22.
(21) Hayek, K.; Glassl, H.; Gutmann, A.; Leonhard, H.; Prutton, M.; Tear, S. P.; Weltoncook, M. R. *Surf. Sci.* **1985**, *152*, 419−425.
(22) Hayek, K.; Glassl, H.; Gutmann, A.; Leonhard, H.; Prutton, M.; Tear, S. P.; Weltoncook, M. R. *Surf. Sci.* **1986**, *175*, 535−550.
(23) Sung, Y. E.; Chrzanowski, W.; Zolfaghari, A.; Jerkiewicz, G.; Wieckowski, A. *J. Am. Chem. Soc.* **1997**, *119*, 194−200.
(24) Sung, Y. E.; Chrzanowski, T.; Wieckowski, A.; Zolfaghari, A.; Blais, S.; Jerkiewicz, G. *Electrochim. Acta* **1998**, *44*, 1019−1030.
(25) Perdereau, M.; Oudar, J. *Surf. Sci.* **1970**, *20*, 80−98.
(26) Demuth, J. E.; Jepsen, D. W.; Marcus, P. M. *Phys. Rev. Lett.* **1974**, *32*, 1182−1185.
(27) Ruan, L.; Stensgaard, I.; Besenbacher, F.; Laegsgaard, E. *J. Vac. Sci. Technol., B* **1994**, *12*, 1772−1775.
(28) Li, L. F.; Totir, D.; Chottiner, G. S.; Scherson, D. A. *J. Phys. Chem. B* **1998**, *102*, 8013−8016.
(29) Foord, J. S.; Reynolds, A. E. *Surf. Sci.* **1985**, *164*, 640−648.
(30) Wong, K. C.; Liu, W.; Saidy, M.; Mitchell, K. A. R. *Surf. Sci.* **1996**, *345*, 101−109.
(31) Yoon, H. A.; Salmeron, M.; Somorjai, G. A. *Surf. Sci.* **1998**, *395*, 268−279.
(32) Maca, F.; Scheffler, M.; Berndt, W. *Surf. Sci.* **1985**, *160*, 467−474.
(33) Patterson, C. H.; Lambert, R. M. *Surf. Sci.* **1987**, *187*, 339−358.
(34) Forbes, J. G.; Gellman, A. J.; Dunphy, J. C.; Salmeron, M. *Surf. Sci.* **1992**, *279*, 68−78.
(35) Dhanak, V. R.; Shard, A. G.; Cowie, B. C. C.; Santoni, A. *Surf. Sci.* **1998**, *410*, 321−329.
(36) Speller, S.; Rauch, T.; Bomermann, J.; Borrmann, P.; Heiland, W. *Surf. Sci.* **1999**, *441*, 107−116.
(37) Kelemen, S. R.; Fischer, T. E. *Surf. Sci.* **1979**, *87*, 53−68.
(38) Dennert, R.; Sokolowski, M.; Pfnur, H. *Surf. Sci.* **1992**, *271*, 1−20.
(39) Heuer, D.; Muller, T.; Pfnur, H.; Kohler, U. *Surf. Sci.* **1993**, *297*, L61−L67.
(40) Jurgens, D.; Held, G.; Pfnur, H. *Surf. Sci.* **1994**, *303*, 77−88.
(41) Muller, T.; Heuer, D.; Pfnur, H.; Kohler, U. *Surf. Sci.* **1996**, *347*, 80−96.
(42) Touzov, I.; Gorman, C. B. *Langmuir* **1997**, *13*, 4850−4854.
(43) Cabibil, H.; Lin, J. S.; Kelber, J. A. *Surf. Sci.* **1997**, *382*, L645−L651.
(44) Somorjai, G. A. *J. Catal.* **1972**, *27*, 453.
(45) Barbouth, N.; Salame, M. *J. Catal.* **1987**, *104*, 240−245.
(46) Owens, W. T.; Rodriguez, N. M.; Baker, R. T. K. *Catal. Today* **1994**, *21*, 3−22.
(47) Aguinaga, A.; Montes, M.; Malet, P.; Capitan, M. J.; Carrizona, I.; Odriozola, J. A. *Appl. Catal., A* **1994**, *110*, 197−205.
(48) Foresti, M. L.; Pezzatini, G.; Cavallini, M.; Aloisi, G.; Innocenti, M.; Guidelli, R. *J. Phys. Chem. B* **1998**, *102*, 7413−7420.
(49) Innocenti, M.; Pezzatini, G.; Forni, F.; Foresti, M. L. *J. Electrochem. Soc.* **2001**, *148*, C357−C362.
(50) Cecconi, T.; Atrei, A.; Bardi, U.; Forni, F.; Innocenti, M.; Loglio, F.; Foresti, M. L.; Rovida, G. *J. Electron Spectrosc. Relat. Phenom.* **2001**, *114*, 563−568.
(51) Demir, U.; Shannon, C. *Langmuir* **1996**, *12*, 6091−6097.
(52) Gichuhi, A.; Boone, B. E.; Demir, U.; Shannon, C. *J. Phys. Chem. B* **1998**, *102*, 6499−6506.
(53) Gichuhi, A.; Shannon, C.; Perry, S. S. *Langmuir* **1999**, *15*, 5654−5661.
(54) Torimoto, T.; Obayashi, A.; Kuwabata, S.; Yasuda, H.; Mori, H.; Yoneyama, H. *Langmuir* **2000**, *16*, 5820−5824.
(55) Torimoto, T.; Nagakubo, S.; Nishizawa, M.; Yoneyama, H. *Langmuir* **1998**, *14*, 7077−7081.
(56) Torimoto, T.; Obayashi, A.; Kuwabata, S.; Yoneyama, H. *Electrochem. Commun.* **2000**, *2*, 359−362.
(57) Gregory, B. W.; Stickney, J. L. *J. Electroanal. Chem.* **1991**, *300*, 543−561.
(58) Stickney, J. L. In *Electroanalytical Chemistry A Series of Advances*; Bard, A. J., Rubinstein, I., Eds.; Marcel Dekker: New York, 1999; Vol. 21, p 75.
(59) Stickney, J. L. In *Advances in Electrochemical Science and Engineering*; Kolb, D. M., Alkire, R., Eds.; Wiley-VCH: Weinheim, 2002; Vol. 7, pp 1−107.
(60) Goodman, C. H. L.; Pessa, M. V. *J. Appl. Phys.* **1986**, *60*, R65−R81.
(61) Kuech, T. F.; Dapkus, P. D.; Aoyagi, Y. *Atomic Layer Growth and Processing*; Materials Research Society: Pittsburgh, PA, 1991; Vol. 222.
(62) Tischler, M. A.; Bedair, S. M. *J. Cryst. Growth* **1986**, *77*, 89−94.
(63) Niinisto, L.; Leskela, M. *Thin Solid Films* **1993**, *225*, 130.
(64) Kolb, D. M. In *Advances in Electrochemistry and Electrochemical Engineering*; Gerischer, H., Tobias, C. W., Eds.; Wiley & Sons: New York, 1978; Vol. 11, p 125.
(65) Juttner, K.; Lorenz, W. J. *Z. Phys. Chem. (Wiesbaden)* **1980**, *122*, 163−185.
(66) Adzic, R. R. In *Advances in Electrochemistry and Electrochemical Engineering*; Gerischer, H., Tobias, C. W., Eds.; 1984; Vol. 13, pp 159−260.
(67) Niece, B. K.; Gewirth, A. A. *Langmuir* **1997**, *13*, 6302−6309.
(68) Zou, S. Z.; Weaver, M. J. *J. Phys. Chem. B* **1999**, *103*, 2323−2326.
(69) Colletti, L. P.; Flowers, B. H.; Stickney, J. L. *J. Electrochem. Soc.* **1998**, *145*, 1442−1449.
(70) Colletti, L. P.; Stickney, J. L. *J. Electrochem. Soc.* **1998**, *145*, 3594−3602.
(71) Huang, B. M.; Colletti, L. P.; Gregory, B. W.; Anderson, J. L.; Stickney, J. L. *J. Electrochem. Soc.* **1995**, *142*, 3007−3016.
(72) Lister, T. E.; Colletti, L. P.; Stickney, J. L. *Isr. J. Chem.* **1997**, *37*, 287−295.
(73) Forni, F.; Innocenti, M.; Pezzatini, G.; Foresti, M. L. *Electrochim. Acta* **2000**, *45*, 3225−3231.
(74) Pezzatini, G.; Caporali, S.; Innocenti, M.; Foresti, M. L. *J. Electroanal. Chem.* **1999**, *475*, 164−170.
(75) Murase, K.; Watanabe, H.; Mori, S.; Hirato, T.; Awakura, Y. *J. Electrochem. Soc.* **1999**, *146*, 4477−4484.
(76) Murase, K.; Uchida, H.; Hirato, T.; Awakura, Y. *J. Electrochem. Soc.* **1999**, *146*, 531−536.
(77) Murase, K.; Honda, T.; Yamamoto, M.; Hirato, T.; Awakura, Y. *J. Electrochem. Soc.* **2001**, *148*, C203−C210.
(78) Murase, E.; Watanabe, H.; Uchida, H.; Hirato, T.; Awakura, Y. *Electrochemistry* **1999**, *67*, 331−335.
(79) Stickney, J. L.; Wade, T. L.; Flowers, B. H. *Abstr. Pap.—Am. Chem. Soc.* **1999**, *217*, 147-ANYL.
(80) Wade, T. L.; Ward, L. C.; Maddox, C. B.; Happek, U.; Stickney, J. L. *Electrochem. Solid State Lett.* **1999**, *2*, 616−618.

threefold hollow binding sites. At more negative potentials the Au(111) lattice was imaged, indicating desorption of sulfur atoms from the surface. At potentials positive of −0.1 V, a structure composed of rectangular eight-member sulfur rings was observed. Using surface-enhanced Raman spectroscopy (SERS), further evidence for the existence of S_8 rings and other polysulfides was obtained at the onset of bulk sulfur layer formation.[81] Demir and Shannon have also observed the $(\sqrt{3} \times \sqrt{3})R30°$ unit cell on Au(111),[12] as have Salvarezza and co-workers.[14−16]

Sulfur layer deposition on Ag(111) from aqueous Na_2S has been studied by Foresti and co-workers.[82] Prior to bulk deposition of sulfur, two ordered structures were observed using EC-STM: a $^1/_3$ ML $(\sqrt{3} \times \sqrt{3})R30°$ structure and a $^3/_7$ ML $(\sqrt{7} \times \sqrt{7})R19°$ structure. Hatchett and White also investigated sulfur electrodeposition on Ag(111) with EQCM and STM.[83,84] The reversible adsorption of HS^- was observed prior to the formation of a Ag_2S adlayer.

Somorjai et al. performed AES, LEED, and STM studies of sulfur layers on the Rh(111) surface.[31] Ordered sulfur structures were obtained by gas-phase deposition at room temperature followed by substrate heating. Sharp LEED patterns were observed, indicating a number of unit cells with varying coverages, from $^1/_3$ to $^3/_4$ ML, including $(\sqrt{3} \times \sqrt{3})R30°$, c$(\sqrt{3} \times 7)$rect, c$(4 \times 2)$, (4×4), and (7×7). Somorjai and co-workers also examined sulfur structures on Pt(111) by LEED and STM,[85] where $^1/_4$ ML (2×2), $^1/_3$ ML $(\sqrt{3} \times \sqrt{3})R30°$, and $^3/_7$ ML c$(7 \times \sqrt{3})$rec structures were observed.

The formation of S layers has also been studied via UHV-EC, beginning with the adsorption of S on Pt(111) from a sulfide solution[86] and continuing with studies by Wieckowski et al.[23,24] Exposing the Pt crystal to a 1 mM Na_2S solution at open circuit produced sulfur layers that were slowly stripped in sulfuric acid, yielding a number of ordered structures depending on the amount of sulfur oxidized to sulfate. Using LEED and AES, a full coverage (1×1) was observed prior to stripping any deposited sulfur. After one cycle in sulfuric acid a $^1/_2$ ML c(2×2) structure was observed, and after two cycles a $^1/_3$ ML $(\sqrt{3} \times \sqrt{3})R30°$ structure was observed.

This report describes EC-STM,[87] UHV-EC,[88] and thin layer electrochemistry (TLEC)[89,90] studies of S atomic layers formed from sulfide (K_2S) and thiosulfate ($Na_2S_2O_3$) precursors, with the intent of exploring conditions for the electrochemical formation of sulfur based compound semiconductors.

Experimental Section

The experimental arrangements used for EC-STM,[91] UHV-EC,[92] and TLEC[93] experiments have been described elsewhere. For EC-STM experiments, solutions were composed of 0.2 mM K_2S (Atomergic Chemicals) + 1 mM Na_2SO_4 (Baker Analyzed) and 1.0 mM $Na_2S_2O_3$ (Baker Analyzed) + 1.0 mM KOH (Baker Analyzed). UHV-EC solutions contained 0.2 mM K_2S without electrolyte, to avoid an emersion layer and 1 mM $Na_2S_2O_3$ adjusted to pH 9.7 with KOH. TLEC solutions contained 1 mM $Na_2S{\cdot}9H_2O$ + 0.1 M KOH + 0.1 M K_2SO_4, and 6 mM $Na_2S_2O_3$ + 0.1 M KOH + 0.1 M K_2SO_4 (Baker Analyzed). Higher electrolyte levels were used in TLEC studies to offset the greater solution resistance due to the cell geometry. All solutions were prepared fresh daily with water from a Nanopure filtration system (>18 MΩ) and purged with N_2 prior to adding the S precursor. Polycrystalline Au wire was used for auxiliary electrodes, and all potentials were referenced to a 3 M Ag/AgCl reference electrode (BAS).

The TLEC consisted of a polished and annealed polycrystalline Au rod (1.17 × 0.0312 cm^2) fitted into a vacuum shrunk Pyrex glass cavity, shaped to hold the Au rod 0.005 cm from the glass wall of the TLEC.[90,94] The electrode surface area was 8.26 cm^2, with a solution volume of 3.0 μL, producing a very large surface area-to-volume ratio. Two holes at the bottom of the TLEC cavity provided a path for solution to enter and exit the cell and also provided electrical conductivity. Solution entered the cavity via capillary action and was expelled by pressurizing with high purity N_2 gas. Solution reservoirs for TLEC experiments were Pyrex H-cells with standard ground glass joints. The TLEC was fitted using a Teflon thermometer adapter. The reference and auxiliary electrodes were housed in a separate compartment, connected via a fine glass frit. Separate H-cells were used for each solution. The potentiostat was built in house and was based on a conventional op-amp design. The Au working electrode was cleaned electrochemically in 1 M H_2SO_4 prior to each experiment. The cleaning cycle consisted of alternating the electrode potential between −0.5 and 1.4 V and rinsing the TLEC compartment 10 times at each potential. This protocol was repeated three times. The cleanliness of the Au electrode was then assessed with a cyclic voltammogram.

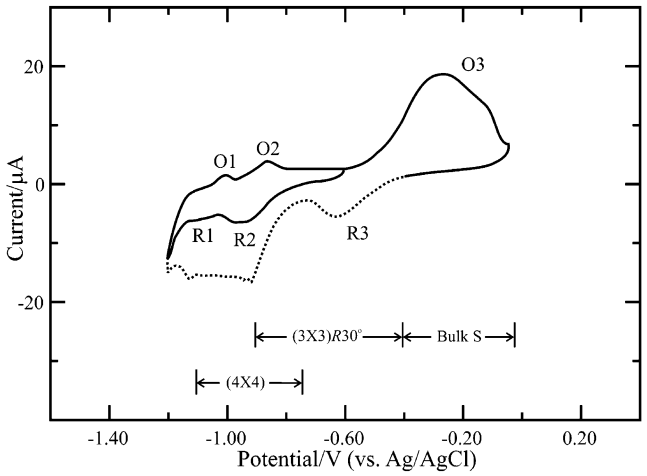

Figure 1. Cyclic voltammogram for a Au(111) electrode in 1 mM Na_2S + 0.10 M K_2SO_4 + 0.10 M KOH. Scan rate = 5 mV/s.

Results and Discussion

Sulfide Voltammetry. Figure 1 shows the voltammetry obtained for a polycrystalline Au TLEC electrode in 1 mM Na_2S + 0.10 M K_2SO_4 + 0.10 M KOH. Scanning negatively from the open circuit potential, −0.60 V, a reduction peak is visible at −0.94 V (R2), followed by a second smaller reduction peak at −1.1 V (R1). The charge associated with these reduction peaks, 100 μC/cm^2, corresponds to desorption of approximately $^1/_3$ ML of sulfur, assuming a two-electron process. This coverage is defined

(81) Gao, X. P.; Zhang, Y.; Weaver, M. J. *Langmuir* **1992**, *8*, 668−672.
(82) Aloisi, G. D.; Cavallini, M.; Innocenti, M.; Foresti, M. L.; Pezzatini, G.; Guidelli, R. *J. Phys. Chem. B* **1997**, *101*, 4774−4780.
(83) Hatchett, D. W.; Gao, X. P.; Catron, S. W.; White, H. S. *J. Phys. Chem.* **1996**, *100*, 331−338.
(84) Hatchett, D. W.; White, H. S. *J. Phys. Chem.* **1996**, *100*, 9854−9859.
(85) Yoon, H. A.; Materer, N.; Salmeron, M.; VanHove, M. A.; Somorjai, G. A. *Surf. Sci.* **1997**, *376*, 254−266.
(86) Stickney, J. L.; Rosasco, S. D.; Salaita, G. D.; Hubbard, A. T. *Langmuir* **1985**, *1*, 66.
(87) Herrero, E.; Buller, L. J.; Abruna, H. D. *Chem. Rev.* **2001**, *101*, 1897−1930.
(88) Soriaga, M. P. *Prog. Surf. Sci.* **1992**, *39*, 325.
(89) Hubbard, A. T.; Anson, F. C. *Electroanal. Chem.* **1971**, *4*, 129.
(90) Hubbard, A. T. *Crit. Rev. Anal. Chem.* **1973**, *3*, 201−242.
(91) Lay, M. D.; Stickney, J. L. *J. Am. Chem. Soc.* **2003**, *125*, 1352−1355.
(92) Varazo, K.; Lay, M. D.; Sorenson, T. A.; Stickney, J. L. *J. Electroanal. Chem.* **2002**, *522*, 104−114.
(93) Christensen, C. R.; Anson, F. C. *Anal. Chem.* **1963**, *35*, 205.
(94) Hubbard, A. T.; Anson, F. C. *Electroanal. Chem.* **1970**, *4*, 129−214.

relative to the number of Au substrate surface atoms. Negative of −1.2 V, there is an increase in reductive current corresponding to solvent decomposition.[95] Upon reversing the scan direction, two small oxidation peaks are visible, with the first at −1.0 V (O1) and the second at −0.86 V (O2). The oxidation and reduction peaks appear to be related, with O1 and O2 being the oxidative upd of S, and R1 and R2 being the reductive stripping of S upd.[81,95−100] Scanning further positive, there is a larger oxidation process (O3), due to the oxidation of sulfide to bulk sulfur and polysulfides,[81,95,97,100] beginning at −0.60 V and continuing until 0.0 V.

Reversing the scan direction at 0 V produces a new reduction feature (R3), not present in the initial scan, at −0.60 V (Figure 1). This is the reduction of sulfur species produced during the large oxidation process at O3. It is interesting that R3 is significantly smaller than O3, suggesting that only some of the product of O3 is reduced in R3. The rest of the product formed in O3 appears to be reduced commensurate with the original R2 and R1 peaks, showing less reversibility. In studies of sulfur deposition using a gold rotating ring disk electrode (RRDE), Buckley and Woods found that some soluble polysulfide intermediates formed during the oxidation of sulfide to sulfur and during the reductive dissolution of sulfur.[95] TLEC studies in this group showed that the product of O3 was strongly adsorbed, as rinsing the TLEC cell with blank electrolyte positive of O3 still resulted in the extra reductive current between −0.4 and −1.0 V, during the subsequent negative going scan.

EC-STM and UHV-EC Studies of Sulfide. Two series of sulfide electrodeposition experiments, using EC-STM and UHV-EC, on Au(111) were performed. Electrolyte concentrations in UHV-EC studies were kept very low in order to avoid precipitation of an electrolyte layer that could interfere with analysis upon emersion of the electrode.[101] Additionally, K_2S was used as a source for sulfide, as K has a much higher Auger yield than Na, making it easier to quantify.

For UHV-EC experiments, the clean and ordered Au(111) crystal was immersed in a 0.20 mM K_2S solution for 2 min at fixed potentials between −1.20 and 0.40 V and then emersed. After pumping down the antechamber to UHV pressures, the crystal was transferred to the analysis chamber. Figure 2 is a graph of the S/Au and K/Au Auger peak height ratios as a function of the immersion potential, and Table 1 lists approximate sulfur and potassium coverages, after sensitivity corrections,[102] along with observed LEED patterns.

Experiments performed at −1.00 V revealed little adsorbed sulfur (0.13 ML), which decreased to 0.0 ML at −1.20 V, where LEED showed a (1 × 1) pattern similar to that obtained for the clean gold surface before immersion. Between −0.80 V and −0.40 V a $^1/_3$ coverage

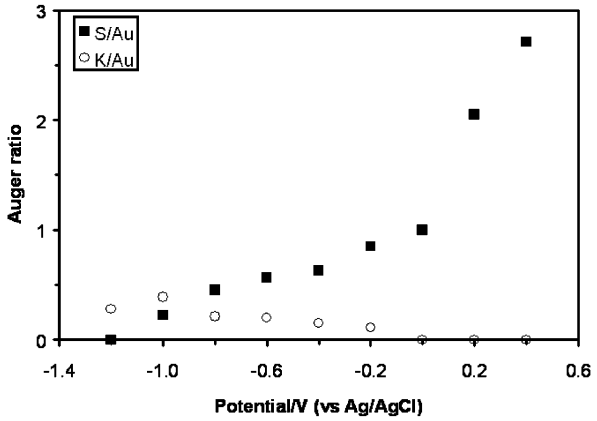

Figure 2. Graph of S/Au and K/Au Auger ratios as a function of immersion potential for a Au(111) electrode in 0.2 mM K_2S.

Table 1. Sulfur and Potassium Coverages with LEED Patterns as a Function of Immersion Potential from 0.20 mM K_2S

potential/V	sulfur coverage/ML	potassium coverage/ML	LEED pattern
0.40	1.60	0	(2 × 2)
0.20	1.21	0	(2 × 2)
0	0.59	0	(2 × 2)
−0.20	0.50	0.06	(2 × 2)
−0.40	0.37	0.09	$(\sqrt{3} \times \sqrt{3})R30°$
−0.60	0.33	0.12	$(\sqrt{3} \times \sqrt{3})R30°$
−0.80	0.27	0.12	$(\sqrt{3} \times \sqrt{3})R30°$
−1.0	0.13	0.23	(1 × 1)
−1.2	0	0.17	(1 × 1)

$(\sqrt{3} \times \sqrt{3})R30°$-S structure was observed by LEED. As noted in the Introduction, the $(\sqrt{3} \times \sqrt{3})R30°$-S structure has been observed previously in aqueous solutions on Au(111),[12,14,15,51,103] as well as Ag(111)[48,82] and Pt(111).[23,24] The $(\sqrt{3} \times \sqrt{3})R30°$ sulfur structure has also been formed by vapor-phase deposition on Pt(111),[17,19,85,104] Rh(111),[31] and Pd(111).[35,36] Additionally, it has been observed in the adsorption of Se on Au(111), and a closely related structure has been observed for Te adsorption on Au(111).[105,106]

In EC-STM studies, a $^1/_3$ ML $(\sqrt{3} \times \sqrt{3})R30°$-S structure was observed at potentials between −0.85 V and −0.40 V (Figure 3a). The various single atom defects present were evidence of the dynamic nature of the adlayer. The density of these defects decreased as the potential for bulk S deposition was approached, with the structure becoming solidly packed just before bulk sulfide oxidation started.

To elucidate the coordination site of adsorbed S atoms, a series of potential step experiments were performed; the $(\sqrt{3} \times \sqrt{3})R30°$-S structure was deposited at −0.85 V, and then the potential was stepped to −0.90 V, to reductively strip the S atoms. If this was carried out during the course of a micrograph, the Au lattice below the S adlayer was exposed and the adsorption locations were determined to be threefold hollow sites (Figure 3b). The first two circles from the top of Figure 3b show full S adatoms, while the third circle shows a partial S atom because it desorbed during the imaging process. The bottom two circles indicate that the S adlayer occupied threefold hollow sites on the Au(111) lattice. There are

(95) Buckley, A. N.; Hamilton, I. C.; Woods, R. *J. Electroanal. Chem.* **1987**, *216*, 213−227.
(96) Hamilton, I. C.; Woods, R. *J. Appl. Electrochem.* **1983**, *13*, 783−794.
(97) Briceno, A.; Chander, S. *J. Appl. Electrochem.* **1990**, *20*, 506−511.
(98) Briceno, A.; Chander, S. *J. Appl. Electrochem.* **1990**, *20*, 512−517.
(99) Lezna, R. O.; Detacconi, N. R.; Arvia, A. J. *J. Electroanal. Chem.* **1990**, *283*, 319−336.
(100) Colletti, L. P.; Teklay, D.; Stickney, J. L. *J. Electroanal. Chem.* **1994**, *369*, 145−152.
(101) Zei, M. S.; Scherson, D.; Lehmpfuhl, G.; Kolb, D. M. *J. Electroanal. Chem.* **1987**, *229*, 99−105.
(102) Davis, L. E.; MacDonald, N. C.; Palmberg, P. W.; Riach, G. E.; Weber, R. E. *Handbook of Auger Electron Spectroscopy*; Physical Electronics Division, Perkin-Elmer Corporation: Eden Prairie, MN, 1978.
(103) McCarley, R. L.; Kim, Y. T.; Bard, A. J. *J. Phys. Chem.* **1993**, *97*, 211−215.
(104) Benard, J.; Oudar, J.; Barbouth, N.; Margot, E.; Berthier, Y. *Surf. Sci.* **1979**, *88*, L35−L41.
(105) Lister, T. E.; Stickney, J. L. *J. Phys. Chem.* **1996**, *100*, 19568−19576.
(106) Sorenson, T. A.; Lister, T. E.; Huang, B. M.; Stickney, J. L. *J. Electrochem. Soc.* **1999**, *146*, 1019−1027.

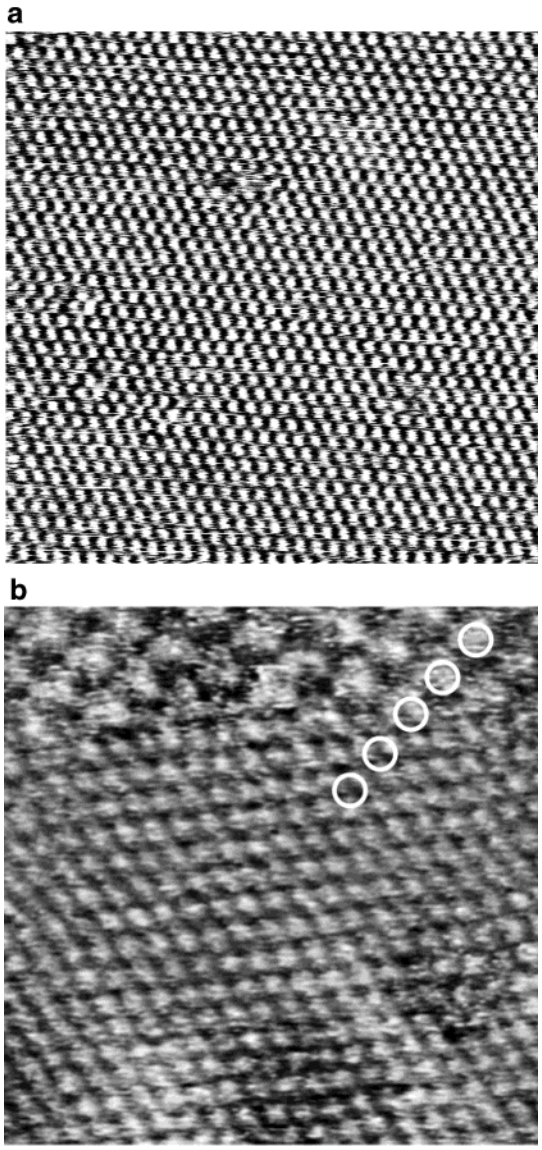

Figure 3. (a) $^1/_3$ coverage $(\sqrt{3} \times \sqrt{3})R30°$-S structure observed at −0.70 V vs 3 M Ag/AgCl. The scan size is 15 × 15 nm^2. (b) S stripping from the Au(111) lattice as the potential was stepped from −0.85 to −0.90 V vs Ag/AgCl in 0.2 K_2S + 1 mM Na_2SO_4. Threefold sites can be assigned to the S atoms. The scan size is 5 × 5 nm^2.

other indications in the literature that low coverages of chalcogenides deposit in threefold hollow sites on Au.[107−109] Previous results have shown that when the chalcogenide atoms are farther apart than their van der Waals diameter, they form simple unit cells, such as a $(\sqrt{3} \times \sqrt{3})R30°$ structure. The positions of the atoms are dictated by high coordinate sites on the Au substrate and interchalcogenide repulsion.[110,111] Conversely, as the coverages increase and the chalcogenide atoms begin to touch, interchalcogenide bonds are structure controlling and rings, chains, or clusters are formed.

(107) Dubois, L. H.; Nuzzo, R. G. *Annu. Rev. Phys. Chem.* **1992**, *43*, 437−463.
(108) Nuzzo, R. G.; Zegarski, B. R.; Dubois, L. H. *J. Am. Chem. Soc.* **1987**, *109*, 733−740.
(109) Sellers, H.; Ulman, A.; Shnidman, Y.; Eilers, J. E. *J. Am. Chem. Soc.* **1993**, *115*, 9389−9401.
(110) Sorenson, T. A.; Lister, T. E.; Huang, B. M.; Stickney, J. L. *J. Electrochem. Soc.* **1999**, *146*, 1019−1027.
(111) Sorenson, T. A.; Varazo, K.; Suggs, D. W.; Stickney, J. L. *Surf. Sci.* **2001**, *470*, 197−214.

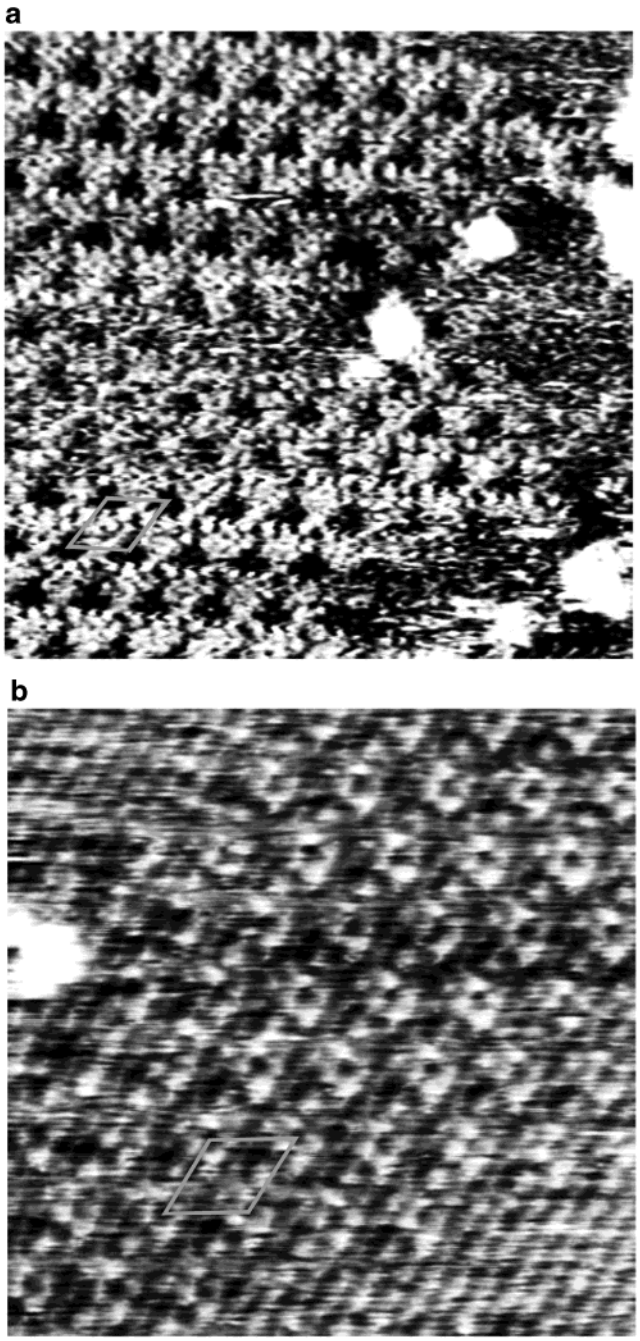

Figure 4. STM micrographs of $(3\sqrt{3} \times 3\sqrt{3})R30°$-S adlayers imaged in 0.2 mM K_2S + 1 mM Na_2SO_4 at (a) −0.40 V vs 3 M Ag/AgCl (the scan size is 15 × 15 nm^2) or (b) −0.58 V vs 3 M Ag/AgCl (the scan size is 10 nm^2).

At this point, it is important to draw a distinction between the first S deposits formed on a clean ordered Au(111), starting from −1.2 V, and initiation of S deposition on a Au(111) substrate from which bulk S has just been stripped. If a well ordered, annealed, electrode is used and the deposition is started from −1.2 V, the first structure observed was the $(\sqrt{3} \times \sqrt{3})R30°$-S one, at $^1/_3$ ML. This structure remained until potentials between −0.5 and −0.4 V, at which point two $(3\sqrt{3} \times 3\sqrt{3})R30°$-S adlayers formed (Figure 4). From the voltammetry (Figure 1), this corresponds to initiation of the bulk sulfide oxidation process O3. The coverage corresponding to the $(3\sqrt{3} \times 3\sqrt{3})R30°$-S adlayer is difficult to discern from the low resolution of the images; however, the structure does appear to be composed of a higher density of S atoms

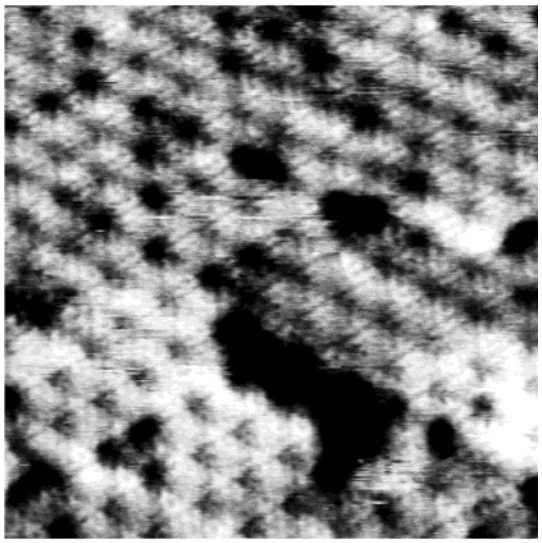

Figure 5. STM micrograph of a (4 × 4)-S adlayer captured at −0.90 V vs 3 M Ag/AgCl. The scan size is 15 × 15 nm^2.

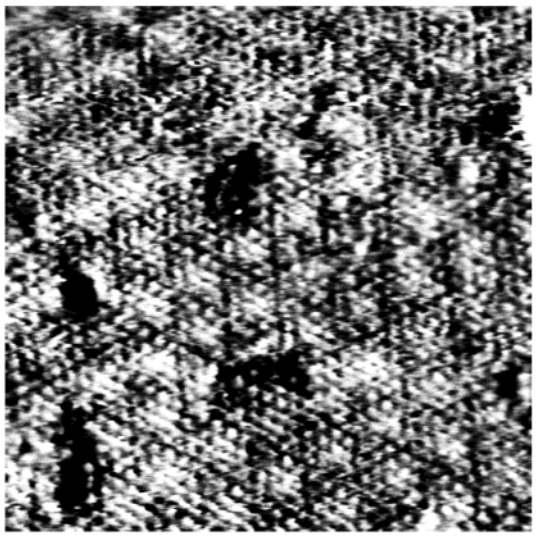

Figure 6. Templated Au(111) surface imaged at −1.1 V vs 3 M Ag/AgCl, after the desorption of the (4 × 4)-S adlayer. The scan size is 12 × 12 nm^2.

than the ($\sqrt{3} \times \sqrt{3}$)*R*30°-S structure. Subsequent deposition, into O3, results in surface roughening, as bulk S or polysulfides were deposited.

One of the major questions in this work concerns the nature of the bulk deposit. One model is that as bulk deposits are formed, the first step is formation of a higher density S layer on the surface, such as a layer of S_8 rings, 0.9 ML.[112−114] The ($3\sqrt{3} \times 3\sqrt{3}$)*R*30°-S structure may be a precursor to such a layer. Bulk deposits of S or polysulfides are deposited on top of this layer, probably in the form of S_8 rings or chains, consistent with the bulk structure of S.[115]

A subsequent reductive scan resulted in the return of the ($\sqrt{3} \times \sqrt{3}$)*R*30°-S structure, at potentials near −0.5 V. This corresponded to the new reductive feature in Figure 1 (R3). R3 appears to be related to selective reduction of some of the bulk S or polysulfides formed in O3. As noted previously, the rest of the species formed in O3 are reduced at considerable overpotentials, near R1 and R2. Given the model structure proposed in the last paragraph, it may be that R3 is the result of reduction of the compact, S_8, sulfur layer in contact with the Au surface. It is probable that the S_8 layer, 0.9 ML, was converted to the ($\sqrt{3} \times \sqrt{3}$)*R*30°-S structure, $^1/_3$ ML, rather than a clean Au surface, given the stability of the ($\sqrt{3} \times \sqrt{3}$)*R*30°-S structure at these potentials and the fact that the ($\sqrt{3} \times \sqrt{3}$)*R*30°-S structure was observed via EC-STM. The fact that some of the species were only reduced at large overpotentials is consistent with the nature of bulk S, as bulk S is composed of chains and rings of S atoms, held together by van der Waals forces. Thus, these species would not be in direct contact with the surface, making electron transfer more difficult to any bulk S and polysulfides.[81,95,97,100]

In addition to imaging the predominant ($\sqrt{3} \times \sqrt{3}$)*R*30°-S structure, on some select terraces a fairly disordered structure with a (4 × 4) periodicity was imaged. As the potentials were shifted more negative, the atomic basis of this (4 × 4) periodicity became better resolved (Figure 5). The (4 × 4) structure was still not well defined, but it was characterized by an essentially (1 × 1) array of atoms, with a periodic array of pits. On plateaus where the ($\sqrt{3} \times \sqrt{3}$)*R*30°-S structure existed, only the clean unreconstructed Au(111) surface was observed. Conversely, the (4 × 4) structure, on its select terraces, persisted. In fact, the (4 × 4) structure remained until potentials near −1.1 V, where the Au surface atoms left behind appeared to retain a template of the (4 × 4) structure (Figure 6).

It is known that the adsorption of chalcogenides causes changes, or reconstructions, in the underlying Au surface: the pits and roughening discussed in the above, as well as from surface X-ray diffraction (SXRD).[116,117] It is likely that when high coverage chalcogenide layers are formed, the interchalcogenide bonding, together with the bonding to the Au surface, result in strain which is relieved by surface reconstructions. Thus, it is understandable that when bulk S starts to deposit, the surfaces may become templated. Then during the subsequent reductive scan, most of this strain is relieved when the high density structure is reduced to the low density ($\sqrt{3} \times \sqrt{3}$)*R*30°-S structure. Evidently, some of this bulk remains and is only slowly reduced from the surface, accounting for the persistence of the (4 × 4) unit cell in the Au lattice, even when all the S is removed (Figure 6).

Figure 7, captured at −0.90 V, shows an image of the Au(111) substrate where the ($\sqrt{3} \times \sqrt{3}$)*R*30°-S structure had just been stripped. There is no evidence of the (4 × 4)-S or any other S adlayer at this potential, though some pitting is evident. This again suggests the tendency for sulfur atomic layers to reconstruct the Au substrate surface atoms.

If the potential was scanned positively a second time, the ($\sqrt{3} \times \sqrt{3}$)*R*30°-S adlayer again covered the majority of the surface where the (4 × 4) template was not present. However, on terraces initially covered by the (4 × 4) template, a new structure appeared (Figure 8). The lower terrace in Figure 8 displays a well ordered ($\sqrt{3} \times \sqrt{3}$)*R*30°-S structure, but the upper terrace, which had initially supported the (4 × 4) template, shows a new (4 × 4) structure. Although the top structure in Figure 8

(112) Gao, X.; Zhang, Y.; Weaver, M. J. *Langmuir* **1992**, *8*, 668−672.
(113) Gao, X.; Zhang, Y.; Weaver, M. J. *J. Phys. Chem.* **1992**, *96*, 4156−4159.
(114) Kolb, D. M. *Electrochim. Acta* **2000**, *45*, 2387−2402.
(115) Greenwood, N. N.; Earnshaw, A. *Chemistry of the Elements*; Pergamon Press: Oxford, U.K., 1984.
(116) Poirier, G. E.; Tarlov, M. J. *J. Phys. Chem.* **1995**, *99*, 10966−10970.
(117) Alves, C. A.; Smith, E. L.; Porter, M. D. *J. Am. Chem. Soc.* **1992**, *114*, 1222−1227.

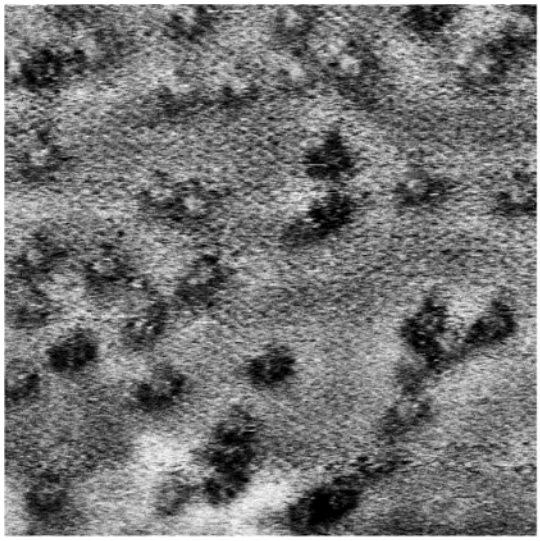

Figure 7. Au(111) surface, at −0.9 V vs 3 M Ag/AgCl, after the cathodic desorption of S. The scan size is 15 × 15 nm^2.

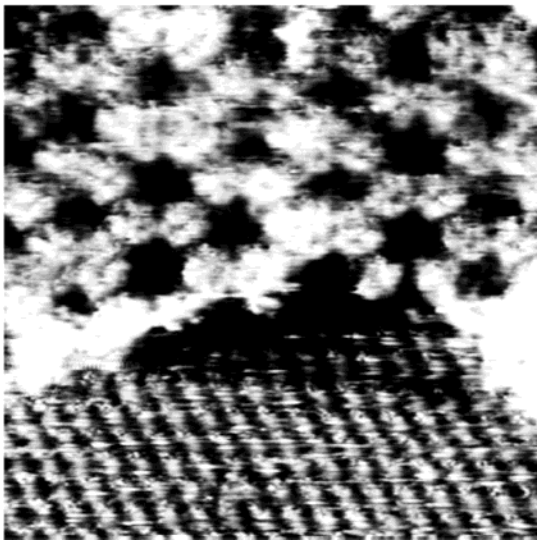

Figure 8. ($\sqrt{3} \times \sqrt{3}$)*R*30°-S (bottom) and (4 × 4)-S (top) structures existing concomitantly at −0.70 V vs 3 M Ag/AgCl. The scan size is 8 × 8 nm^2.

is not atomically resolved, previous results by Salvarezza et al.[118] displayed a similar image, described as a S_3 structure, at similar potentials. The average interatomic spacing in their image was similar to that for the ($\sqrt{3} \times \sqrt{3}$)*R*30°-S structure, 0.5 nm, though the triplets appeared to have a slightly shorter inter-sulfur spacing, 0.4 nm, but not close to the 0.21 nm found for elemental S_8 rings.

In UHV-EC emersion experiments, between −0.80 and −0.40 V, the S/Au Auger ratio was relatively constant and a ($\sqrt{3} \times \sqrt{3}$)*R*30° diffraction pattern was visible with LEED, as noted above (Table 1). The fact that there was no evidence for the (4 × 4) structure was consistent with the idea that it existed on a small portion of the surface. Over this same potential range, significant changes were seen on the majority of terraces using EC-STM. For instance, at the lowest potentials, near −0.8 V, only the Au(111) corrugation was imaged and the step edges were frizzy, indicating the mobility of Au atoms at the step edge (Figure 9). As the potential was slowly shifted positively, domains of S atoms became visible, but only at the step edge. Specifically, S atoms appeared to nucleate on the edge and grow back across the upper plateau. This greatly decreased the frizziness of the edges, as the domains of S limited the mobility of the Au surface atoms. It is interesting that the UHV-EC emersion experiments did not show a significant change in the coverage of adsorbed S. One explanation is that the majority of S composing the ($\sqrt{3} \times \sqrt{3}$)*R*30°-S structure was on the surface, even in Figure 9a, but the atoms displayed a high degree of mobility. Then, during the emersion process, the domains of the ($\sqrt{3} \times \sqrt{3}$)*R*30°-S adlayer formed and grew. The actual increase in S coverage was minor, as most of it was already present, as seen by Auger spectroscoy (Table 1).

It is notable that the K signal is largest at negative potentials, where the sulfur coverage was lowest (Figure 2). This may result from a surface excess trapped in the emersion layer, due to the electrode potential being significantly below the point of zero charge (pzc). The K/Au ratio decreased as the potential was increased. In the range where the ($\sqrt{3} \times \sqrt{3}$)*R*30°-S structure is observed with STM, plateaus in the coverages of both S and K were observed. At still higher potentials, where bulk S begins to deposit, the K coverage decreased to zero. EC-STM studies give no indication of specifically adsorbed cations in the ($\sqrt{3} \times \sqrt{3}$)*R*30°-S structure, but electrodeposited K or even desolvated K^+ ions would not be expected on the surface at these potentials.[12,14,15,51,103] Previous UHV-EC immersion experiments involving K_2S on Pt(111) resulted only in a diffuse LEED pattern, though a ($\sqrt{3} \times \sqrt{3}$)*R*30° pattern was observed after annealing to 400 °C.[119,120] Auger analysis revealed a strong sulfur signal and a small potassium signal, similar in magnitude to those in the present study. Adsorbed K was attributed to the incomplete neutralization of sulfide ions by oxidative adsorption of S layers deposited on Pt(111) from sulfide solutions, where S was found to have some anionic character on the basis of core-level electron energy loss (CEELS) and X-ray photoelectron spectroscopy (XPS) data.[23] Again, there was no indication that the presence of potassium influenced the observed sulfur structures. At 0 V, there was no detectable potassium signal in the Auger spectrum, suggesting the bulk sulfur layer was neutral.

UHV-EC immersion experiments performed between −0.20 and 0.40 V revealed only a diffuse (2 × 2) unit cell, not previously reported for S adlayers. A clear (2 × 2) adlayer was not observed with EC-STM in the sulfide solutions, although one was observed in thiosulfate solution using EC-STM and UHV-EC (discussed below). The diffuseness of the LEED patterns suggested significant disorder, so the crystal was gently annealed, producing a complex pattern and a sight decrease in the S coverage from AES. Further annealing produced the $^1/_3$ coverage ($\sqrt{3} \times \sqrt{3}$)*R*30° structure, with more loss of S. This is consistent with the (2 × 2) structure being a higher coverage structure ($^1/_2$ vs $^1/_3$ ML, respectively) than the ($\sqrt{3} \times \sqrt{3}$)*R*30° structure (Table 1). A (2 × 2) structure with 0.5 ML S coverage, formed by electrodeposition on Pt(111), has been reported by Wieckowski et al.[23,24] Similarly, (2 × 2) structures were formed on Pt(111)[85] and Pd(111)[36] by evaporation and subsequent annealing, but with $^1/_4$ ML S coverage in each case.

(118) Vericat, C.; Vela, M. E.; Andreasen, G. A.; Salvarezza, R. C.; Borgatti, F.; Felici, R.; Lee, T. L.; Renner, F.; Zegenhagen, J.; Martin-Gago, J. A. *Phys. Rev. Lett.* **2003**, *90*, art. no.-075506.

(119) Stickney, J. L.; Rosasco, S. D.; Salaita, G. N.; Hubbard, A. T. *Langmuir* **1985**, *1*, 66−71.

(120) Stickney, J. L.; Rosasco, S. D.; Salaita, G. N.; Hubbard, A. T. *Abstr. Pap.—Am. Chem. Soc.* **1984**, *188*, 8-COLL.

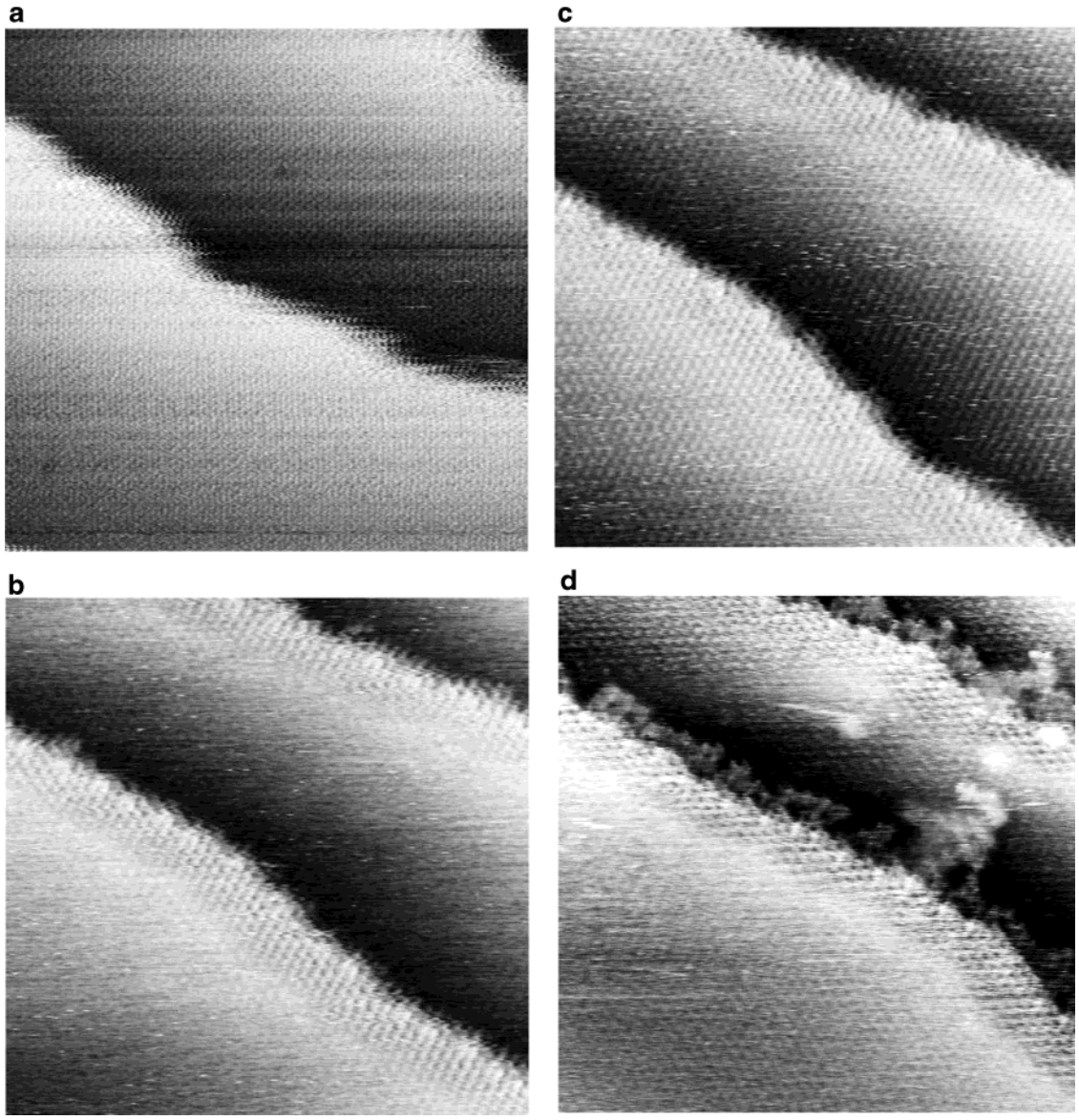

Figure 9. Evolution of the Au(111) step edges during the course of S electrodeposition: (a) fuzzy step at −0.80 V vs 3 M Ag/AgCl; (b) S adsorbed at step edges at −0.73 V; (c) S covering the entire plateau at −0.70 V; (d) nucleation of bulk S at step edges at −0.50 V vs 3 M Ag/AgCl. All images are 20 × 20 nm^2.

At 0.20 V, UHV-EC revealed the S/Au Auger ratio increased sharply, indicating deposition of bulk sulfur. In previous EC-STM studies, Weaver and Salvarezza separately reported the formation of rectangular eight-member ring structures on Au(111) with a sulfur coverage just below 1 ML.[11,14,15] However, no such structures were observed under the conditions used in the present studies, although Se_8 rings have been observed to form on Au(111) by this group.[121,122]

TLEC Quantitative Study of S Stripping. On Au, sulfur is irreversibly oxidized to sulfate in a six-electron process, in acidic media, at positive potentials, and Au oxide formation accompanies this process.[100,123−126] To determine S coverages as a function of potential, a thin layer electrochemical cell was used, where adsorbed S layers were oxidized to sulfate in 1 M sulfuric acid and the charges were corrected for concomitant gold oxidation.[127] A typical experiment began with rinsing the clean Au electrode in a blank solution 10−15 times at −1.30 V to remove any acid remaining from the cleaning cycle. This potential was chosen so that excess protons would be reduced to hydrogen gas, as the Pyrex glass walls of the TLEC cell acted as a dilute pH buffer, after exposure to acid.[100] The blank solution was then flushed from the TLE cavity, and the cell was filled with a sulfide solution at the desired potential. It was held for 60 s to allow adsorption, after which the sulfide solution was expelled and the cell was rinsed with a blank solution at the same potential. Finally, the cell was filled with 1 M H_2SO_4 at 0 V, and the potential was scanned to 1.40 V, during which the S oxidized to sulfate, at potentials greater than 0.80 V.[100,123−126] A second sweep was performed to ensure that all of the sulfur on the electrode had been removed and

(121) Huang, B. M.; Lister, T. E.; Stickney, J. L. *Surf. Sci.* **1997**, *392*, 27.
(122) Lister, T. E.; Colletti, L. P.; Stickney, J. L. *Isr. J. Chem.* **1997**, *37*, 287.
(123) Samec, Z.; Weber, J. *Electrochim. Acta* **1975**, *20*, 403−412.
(124) Wierse, D. G.; Lohrengel, M. M.; Schultze, J. W. *J. Electroanal. Chem.* **1978**, *92*, 121−131.
(125) Vanhuong, C. N.; Parsons, R.; Marcus, P.; Montes, S.; Oudar, J. *J. Electroanal. Chem.* **1981**, *119*, 137−148.
(126) Lamy-Pitara, E.; Barbier, J. *Electrochim. Acta* **1986**, *31*, 717−721.
(127) Colletti, L. P.; Teklay, D.; Stickney, J. L. *J. Electroanal. Chem.* **1994**, *369*, 145.

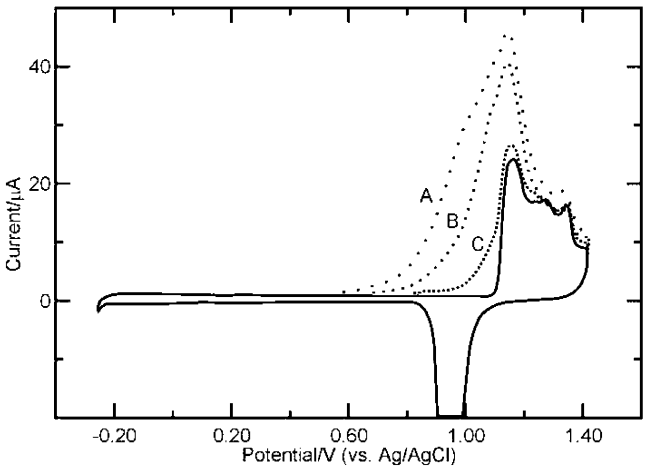

Figure 10. Linear stripping voltammetry of sulfur layers in 1 M H_2SO_4 imposed on the voltammetry for the clean Au electrode (solid line). The scan rate = 5 mV/s. Sulfur was deposited in 1 mM Na_2S + 0.10 M K_2SO_4 + 0.10 M KOH at the following potentials: (A) −0.30 V; (B) −0.50 V; (C) −1.1 V.

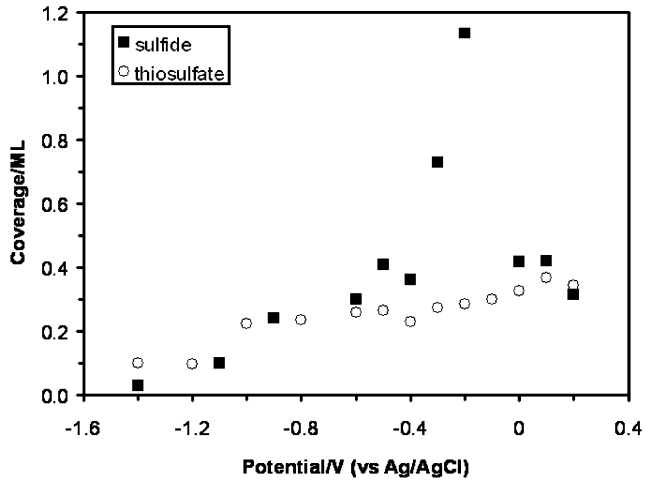

Figure 11. Graph of sulfur coverage, determined from TLEC data as a function of immersion potential from 1 mM Na_2S + 0.10 M K_2SO_4 + 0.10 M KOH, and 1 mM $Na_2S_2O_3$ + 0.10 M K_2SO_4 + 0.10 M KOH solutions.

to determine the charge for gold oxide formation. This procedure was repeated for a range of sulfide adsorption potentials between −1.40 and 0.40 V. Figure 10 shows the linear stripping voltammetry for S oxidation in 1 M H_2SO_4 after adsorption at −0.30 V (a), −0.50 V (b), and −1.10 V (c), as described above. Sulfur oxidation began prior to gold oxide formation and continued until 1.40 V. The clean gold scan was obtained during the second sweep (solid line). The largest stripping charges were observed for sulfur deposited at −0.30 V (a), corresponding to 1.1 ML, consistent with bulk sulfur deposition.[81,95−99,128] At −0.50 V (b), at the base of the bulk sulfide oxidation peak (Figure 1), the sulfur coverage was 0.41 ML, while, at −1.10 V (c), the coverage was 0.10 ML. This was all consistent with the EC-STM and UHV-EC data.

Figure 11 shows S coverage as a function of deposition potential. There is a plateau between −1.0 and −0.60 V, the region where oxidative sulfur upd occurs. From −0.50 to −0.20 V the coverage increases sharply, corresponding to bulk sulfur deposition[81,95−99,128] and polysulfide formation.[95] At potentials more positive than −0.20 V, the coverage decreases. This may be due to the formation of soluble polysulfides by reaction of the sulfur layer with sulfide,[95,129] or the potential may be positive enough to

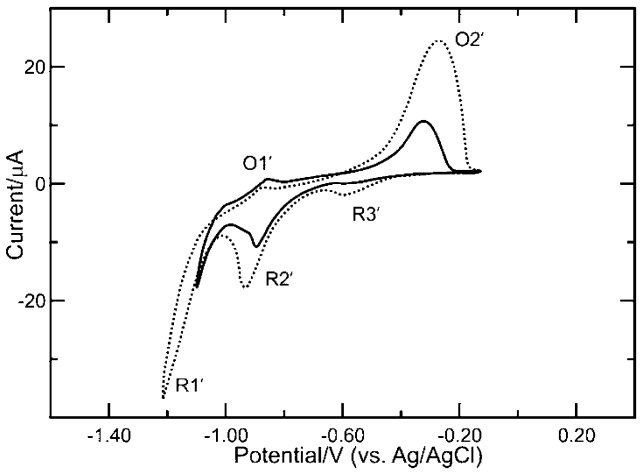

Figure 12. Cyclic voltammogram of a polycrystalline Au electrode in 6 mM $Na_2S_2O_3$ + 0.10 M K_2SO_4 + 0.10 M KOH. The scan rate = 5 mV/s. The first sweep is the solid line, and the second sweep is the dotted line.

facilitate some oxidation of S to sulfate.[124] Negative of −1.1 V the sulfur coverage drops close to zero, where reductive dissolution is expected.

Thiosulfate Voltammetry. Thiosulfate experiments were carried out in alkaline solutions to prevent thiosulfate decomposition.[130−132] Scanning negatively from the open circuit potential (Figure 12), −0.23 V, a reduction peak, R2′, was visible at −0.90 V (the solid line is the first sweep). The measured charge for the peak was 110 $\mu C/cm^2$, corresponding to the reductive dissolution of about $^1/_3$ ML of sulfur. This result is similar to the reductive stripping of sulfur upd seen for peaks R2 and R1 over the same potential region in the sulfide solution (Figure 1). Scanning further negative in the thiosulfate solution, the reduction peak R2′ is followed by a steep increase in reductive current, possibly due to solvent decomposition, at −1.0 V (R1′).[95] Upon reversing the scan, a small oxidation peak, possibly oxidative upd of sulfur (O1′), was observed at −0.88 V. It is noteworthy that thiosulfate results in one anodic upd peak, in contrast to two for sulfide (Figure 1). There is a second oxidation process between −0.60 and −0.20 V (O2′), likely due to the deposition of a bulk sulfur layer. Peak O2′ increased substantially in charge after a second reductive scan, this time to a more negative potential. One explanation is that peak O2′ is the oxidation of sulfide formed by reduction of thiosulfate, at potentials below −1 V. On the second negative sweep (dotted line), there was a new reduction feature (R3′) at −0.60 V that was present only after scanning positively through O2′. This peak is similar to that observed for the second cycle in sulfide, peak R3 (Figure 1). Scanning further negative, the reduction peak at −0.90 V increased in size and shifted slightly negative. Again, this behavior appears directly analogous to the second cycle in sulfide, where there was an initial reduction feature near −0.6 V, followed by increased current at more negative potentials. Again, this is probably due to the partial oxidation of a high density atomic layer of S on the Au, followed by reduction of the weakly bound bulk S which shows slow kinetics. The

(128) Woods, R.; Constable, D. C.; Hamilton, I. C. *Int. J. Miner. Process.* **1989**, *27*, 309−326.
(129) Allen, P. L.; Hickling, A. *Trans. Faraday Soc.* **1957**, *53*, 1626−1635.
(130) Johnston, F.; McAmish, L. *J. Colloid Interface Sci.* **1973**, *42*, 112−119.
(131) Fatas, E.; Herrasti, P.; Arjona, F.; Camarero, E. G.; Medina, J. A. *Electrochim. Acta* **1987**, *32*, 139−148.
(132) Aylmore, M. G.; Muir, D. M. *Miner. Eng.* **2001**, *14*, 135−174.

charge was 210 μC/cm^2 for bulk oxidation (O2′) and 200 μC/cm^2 for the corresponding reductions, suggesting a quantitative process.

In the second cycle (dotted line in Figure 12), the electrode was scanned further negative than was the case in the first dotted scan. In the subsequent positive scan, the upd feature O1′ was essentially the same, while the bulk oxidation feature O2′ more than doubled. In the case of sulfide, the size of the bulk peak appeared to be self-limiting. Self-poisoning in the bulk chalcogenide layer has previously been observed in Se deposition.[133] In the present case, it appears that the bulk peak (O2′) is limited by the extent of the previous reduction process. Explicitly, it appears that the reduction process R1′ includes thiosulfate reduction to sulfide, in addition to solvent decomposition, with the product sulfide being subsequently oxidatively deposited in O2′.

As noted previously, TLEC was used to show that the large oxidation peak at −0.30 V (O3 in Figure 1) in sulfide was due to the deposition of an insoluble elemental sulfur species on the electrode.[100] Similar TLEC experiments were performed with thiosulfate, which showed that the species formed in O2′, probably bulk S or polysulfides, was not soluble and stayed on the surface despite rinsing in the blank solution.

A related experiment was performed to identify the sulfur species undergoing oxidation at −0.30 V. After extensive reduction to −1.2 V and scanning positively through sulfur upd, the solution was again exchanged for the blank, 0.10 M K_2SO_4 + 0.10 M KOH, at −0.65 V, and the scan was then continued in the positive direction to 0 V. Peak O2′ was absent, demonstrating that the species oxidized at −0.30 V (O2′) was a soluble species, likely sulfide, and was rinsed out of the TLEC cavity, precluding bulk sulfur deposition.

The average oxidation state for the sulfur atoms in a thiosulfate molecule is +2, though one may think of the molecule as having sulfur atoms with oxidation states of 0 and +4. Either way, it is known that sulfide can be produced by the reduction of thiosulfate.[115] As mentioned above, the reduction process occurring at −1.0 V is believed to include thiosulfate reduction to sulfide, as O2′ is not visible unless the electrode potential is first scanned below −0.90 V. The open circuit potential in the thiosulfate solution was more positive than that in the corresponding sulfide solution, −0.2 and −0.6 V, respectively. For the sulfide solution, the rest potential was held negative of the potential for bulk sulfide oxidation, while, for thiosulfate, the rest potential was in the range where bulk sulfide oxidation is expected. This suggests that at open circuit in the thiosulfate solution there was no sulfide present to oxidize and thus no redox species in solution to shift the potential more negative, as observed in sulfide solutions. This point is borne out by the EC-STM data below.

The S coverage from thiosulfate follows that from sulfide (Figure 11), until potentials corresponding to the initiation of bulk sulfur formation. At this point, the S coverage in the thiosulfate solution does not dramatically increase, as was the case in the sulfide solutions. This is consistent with the above discussions, as there should be no sulfide in solution, and any elemental sulfur on the surface is probably the result of a surface-limited decomposition of thiosulfate.

EC-STM and UHV-EC Studies of Thiosulfate. At the open circuit potential, −0.2 V, EC-STM revealed a c(4 × 2$\sqrt{3}$) structure (Figure 13). Scanning positively to −0.05 V appeared to result in oxidative desorption of this adlayer, as only the Au(111) lattice was imaged. When the potential was then stepped to −0.88 V and scanned positive again, starting at −0.85 V, a $^1/_3$ coverage ($\sqrt{3} \times \sqrt{3}$)R30° structure, very similar to that observed in the case of sulfide (Figure 3), was observed. This ($\sqrt{3} \times \sqrt{3}$)R30° structure was observed only after stepping the potential to −0.88 V, where thiosulfate appears to be reduced to sulfide. Again, the S appeared to deposit initially at step edges in thiosulfate, as observed in sulfide solutions.

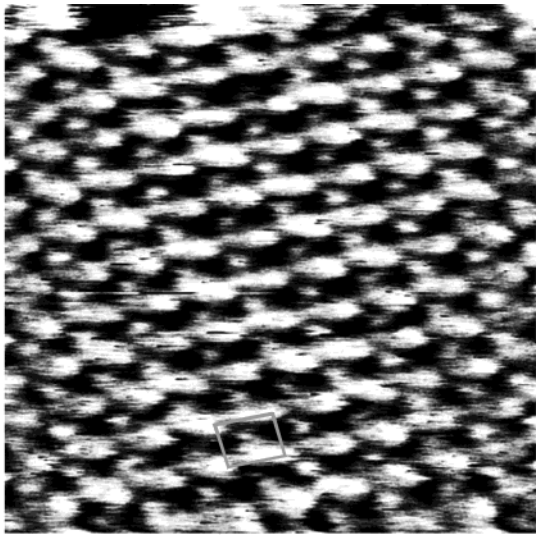

Figure 13. STM micrograph of the c(4 × 2$\sqrt{3}$) structure adsorbed on the Au(111) electrode at −0.15 V vs 3 M Ag/AgCl in 1.0 mM $Na_2S_2O_3$ + 1.0 mM KOH. The scan size is 7.5 × 7.5 nm^2.

Scanning positive to −0.45 V, bulk S began to form. As there was a limited amount of sulfide produced during the negative potential excursion, bulk S did not cover the entire surface, and the ($\sqrt{3} \times \sqrt{3}$)R30°-S was still visible between islands of bulk S. Both adlayers were observed to desorb in one image when the potential was stepped from −0.20 to −0.15 V. This was followed by the reappearance of the Au(111) lattice, suggesting oxidation of adsorbed sulfur at −0.15 V. This concurs with the decrease in S coverage observed for sulfide solutions in TLEC studies at potentials positive of −0.2 V (Figure 11).

Stepping the potential back to −0.45 V, a $^1/_2$ coverage (2 × 2)-S structure (Figure 14) was formed. Instead of single S atoms, as observed in the ($\sqrt{3} \times \sqrt{3}$)R30°-S structure (Figure 3), each unit cell appears to contain one dimmer, with an interatomic distance of just under 0.29 nm. The image shows some distortion, such that the dimers look more like twin ovals, possibly the result of noise or because the dimer atoms were not in stable sites and were mobile upon imaging.

The nature of the (2 × 2) structure is not yet clear. It appears to have a higher coverage than the ($\sqrt{3} \times \sqrt{3}$)R30° structure but not one as high as that of the S_8 adsorbed layer. It appears at potentials associated with bulk S deposition but where some oxidation of S may have occurred. Previously in this report, the nature of bulk S deposits was proposed: an adsorbed layer of a high density S structure, possibly a layer of S_8 rings, under layers of S_8 rings or chains. However, this bulk deposit is not covalently bound to the substrate; it is only held bound via van der Waals forces, the same forces that hold elemental S together. As the oxidation takes place, the

(133) Lister, T. E.; Stickney, J. L. *J. Phys. Chem.* **1996**, *100*, 19568−19576.

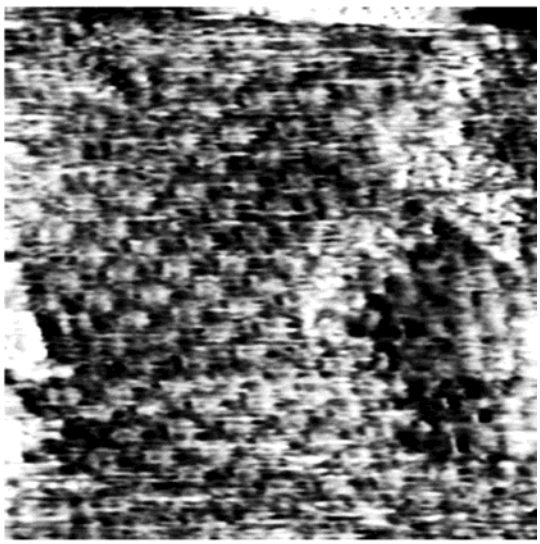

Figure 14. STM micrograph of the (2 × 2) S adlayer observed at −0.65 V vs 3 M Ag/AgCl in 1.0 mM $Na_2S_2O_3$ + 1.0 mM KOH. The scan size is 8 × 8 nm^2.

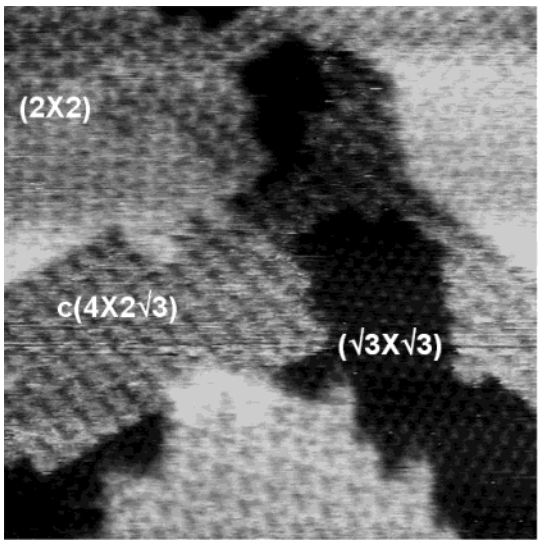

Figure 15. STM image obtained after a long-term polarization experiment of 2 h at −0.15 V vs 3 M Ag/AgCl in 1.0 mM $Na_2S_2O_3$ + 1.0 mM KOH. The scan size is 15 × 15 nm^2.

layer of S in contact with the electrode is the first to oxidize, but it does not completely oxidize; it leaves behind the $(\sqrt{3} \times \sqrt{3})R30°$ structure or possibly the (2 × 2) structure. Oxidation of the majority of the bulk S is an irreversible process; it only slowly oxidizes, as it is not well connected to the electrode. This S_8 oxidation results in the formation of partially oxidized S chains as well as sulfate.

The (2 × 2)-S structure was observed to exist alongside the $(\sqrt{3} \times \sqrt{3})R30°$ structure at −0.65 V, rotated by 30° with respect to it. In a long-term polarization experiment, where a Au(111) electrode was polarized at −0.15 V for 2 h after the creation of sulfide during a negative potential excursion, the three previously mentioned structures were all observed to exist simultaneously, on separate terraces (Figure 15): $c(4 \times 2\sqrt{3})$, $(\sqrt{3} \times \sqrt{3})R30°$, and (2 × 2). This indicates that the processes responsible for forming the (2 × 2)-S structure may be slow in the absence of sufficient sulfide. This also suggests an explanation for the difference between coverage measurements made using TLEC (Figure 11) and those using Auger electron spectroscopy (Figure 2). In the case of Auger measurements, made in a vacuum, high coverages of S are not evident until potentials above 0 V, where oxidation would be expected to start, while there is very little S where bulk would be expected, −0.5 to −0.2 V. This is understandable if the vacuum is considered. Bulk S_8 species would be expected to slowly sublime, leaving only the adsorbed layer.[95] On the other hand, at potentials above −0.2 V, oxidation is starting to occur, and many of the sulfur molecules are at least partially oxidized, probably forming ions, which will not be volatile. Thus, it is only when the partially oxidized species are present that larger amounts of S are seen in Auger studies.

With TLEC, coverage measurements are made after the excess reactant solution is rinsed away. The rinsing will work well on ionic species but will not remove bulk S, as it is neutral. This then explains why the TLEC data agree well with the voltammetry results. At potentials where bulk S is forming, the TLEC coulometry works well. However, at potentials where some of the bulk S is being partially oxidized, the bulk S becomes more soluble and is rinsed from the surface, before coulometry, accounting for the large decrease in coverage above −0.2 V.

Adsorbed thiosulfate results in formation of the $c(4 \times 2\sqrt{3})$ structure. The identity of the species present on the electrode at open circuit in the thiosulfate solutions is not clear (Figure 13). Thiosulfate related species, sulfur, or a combination of the two may be present. Upon emersion, only S is present in the AES spectra, suggesting that if the $c(4 \times 2\sqrt{3})$ structure does contain thiosulfate, it decomposes upon exposure to vacuum, likely with loss of SO_2 and H_2O. An AES study by Freund and co-workers reported similar results for thiosulfate oxidation on gold.[134] The binding energy of S as evinced by XPS was lower than that for bulk elemental sulfur (163.6−164.2 eV)[135−137] and was characteristic of metal sulfides such as Cu_2S (161.5 eV)[138] and CdS (161.7 eV).[139] These XPS results agree with studies of sulfur adsorption on gold by Buckley and co-workers.[95]

Conclusion

Sulfide can be oxidatively deposited on Au(111) substrates from sulfide solutions. At negative potentials, oxidative upd of S occurs, resulting initially in formation of a $^1/_3$ ML $(\sqrt{3} \times \sqrt{3})R30°$-S structure on the lower terrace step edge, and then growing to cover the whole surface. At more positive potentials, bulk S deposition began with formation of a $(3\sqrt{3} \times 3\sqrt{3})R30°$-S structure. After formation of bulk S, and then reduction of the bulk, some terrace displayed a (4 × 4) structure with EC-STM. UHV-EC suggested a $^1/_2$ ML (2 × 2) structure at higher potential, with LEED. The (2 × 2) structure was also observed after emersion from thiosulfate solutions.

In thiosulfate, a $c(4 \times 2\sqrt{3})$ structure was observed at open circuit with EC-STM. At present, the composition is not clear; it is likely adsorbed thiosulfate, S, or both. This structure, however, was not observed with LEED. Additionally, no oxygen was observed with Auger spectroscopy, only S, suggesting this structure decomposed upon

(134) Pedraza, A. M.; Villegas, I.; Freund, P. L.; Chornik, B. *J. Electroanal. Chem.* **1988**, *250*, 443−449.
(135) Lindberg, B. J.; Hamrin, K.; Johansson, G.; Gelius, U.; Fahlman, A.; Nordling, C.; Siegbahn, K. *Phys. Scr.* **1970**, *1*, 286−298.
(136) Mycroft, J. R.; Bancroft, G. M.; McIntyre, N. S.; Lorimer, J. W.; Hill, I. R. *J. Electroanal. Chem. Interfacial Electrochem.* **1990**, *292*, 139−152.
(137) Termes, S. C.; Buckley, A. N.; Gillard, R. D. *Inorg. Chim. Acta* **1987**, *126*, 79−82.
(138) Johansson, L. S.; Juhanoja, J.; Laajalehto, K.; Suoninen, E.; Mielczarski, J. *Surf. Interface Anal.* **1986**, *9*, 501−505.
(139) Bhide, V. G.; Salkalachen, S.; Rastogi, A. C.; Rao, C. N. R.; Hegde, M. S. *J. Phys. D: Appl. Phys.* **1981**, *14*, 1647.

exposure to vacuum. Over time, or with excursions to lower potentials, a $^1/_3$ coverage ($\sqrt{3} \times \sqrt{3})R30°$ structure, very like that formed in sulfide, was observed. At higher potentials, a (2 × 2) structure, that appeared to be composed of S dimers, was observed with EC-STM and LEED. Exposure of the electrode to potentials below −0.9 V resulted in decomposition of thiosulfate, with sulfide formation. Subsequent positive going scans resulted in oxidation of the sulfide to sulfur and formation of a bulk sulfur layer on the electrode at potentials above −0.6 V.

It is interesting that coverage measurements with Auger and thin layer electrochemistry do not agree. However, there are logical reasons for them not to agree, and overall, combining the two methods led to a better understanding of the surface chemistry involved in the present study. In thin layer coulometric studies, partially ionized S_8 chains were rinsed away and not accounted for. In Auger studies, bulk S_8 species sublimed, leaving only the adsorbed layer, unless the chains were partially oxidized and thus not volatile.

Sulfide or thiosulfate may be used to form atomic layers of S. However, a broader range of potentials, over which an atomic layer of S exists, can be obtained using thiosulfate. Thus, it may be more practical to use thiosulfate than sulfide when using EC-ALE to grow sulfur based compounds, as formation of bulk S, and the possibility of three-dimensional growth that would accompany it, would be avoided.

LA034474Y